J|A|C|S
ARTICLES
Published on Web 10/09/2004

Guest Shape-Responsive Fitting of Porous Coordination Polymer with Shrinkable Framework

Ryotaro Matsuda,[†] Ryo Kitaura,[†,‡] Susumu Kitagawa,*[,†] Yoshiki Kubota,[§] Tatsuo C. Kobayashi,[||] Satoshi Horike,[†] and Masaki Takata[⊥]

Department of Synthetic Chemistry and Biological Chemistry, Kyoto University, Katsura, Nishikyo-ku, Kyoto 615-8510, Japan, Department of Environmental Science, Osaka Women's University, Sakai, Osaka 590-0035, Japan, Department of Physics Faculty of Science, Okayama University, Tsushimanaka, Okayama 700-8530, Japan, and JASRI-SPring-8, Koto, Hyogo 679-5198, Japan

Received May 25, 2004; E-mail: kitagawa@sbchem.kyoto-u.ac.jp

Abstract: In situ synchrotron X-ray powder diffraction patterns of porous coordination polymers {[Cu_2(pzdc)$_2$(bpy)]·G} have been measured (pzdc = pyrazine-2,3-dicarboxylate, bpy = 4,4′-bipyridine) (where G = H_2O for **CPL-2** ⊃ **H_2O**, G = benzene for **CPL-2** ⊃ **benzene**, and G = void for the **apohost**). The structures of **apohost** and **CPL-2** ⊃ **benzene** were determined from Rietveld analysis. Adsorption of benzene in the channels induced a remarkable contraction in the crystal (*b* axis; 6.8%, volume; 4.9%), although the channels were occupied by the benzene molecules. This crystal transformation provides a new pore structure that is well suited for benzene molecules, and we denote it as a "shape-responsive fitting" transformation. This type of pore gives rise to a new guideline: frameworks can be composed of flexible motifs that are linked via strong bond and/or stiff motifs that are connected via weaker bonds.

Introduction

Many coordination polymers have been synthesized over the past decade, providing a variety of infinite frameworks of one-, two-, and three-dimensional (3D) motifs containing single and/or polynuclear metal ion cores and linking ligands.[1−7] In particular, porous coordination polymers have attracted the attention of chemists, due to their scientific interest in the creation of nanometer-sized spaces for investigating novel phenomena, as well as for the commercial interest in their application for molecular storage[8−27] and in heterogeneous catalysis.[28−33] These characteristic features are based on these materials' robust open framework, which is ascribed to a permanent porosity in the crystal structure that can accommodate various guest molecules. Using this background, researchers have worked on the synthesis of thermally stable and robust

* Corresponding author. Tel: 81-75-383-2733. Fax: 81-75-383-2732.
[†] Kyoto University.
[‡] Current address: Toyota Central Research and Development Laboratories, Inc., Nagakute, Aichi 480-1192, Japan.
[§] Osaka Women's University.
[||] Okayama University.
[⊥] JASRI-SPring-8.

(1) Kitagawa, S.; Kitaura, R.; Noro, S.-i. *Angew. Chem., Int. Ed.* **2004**, *43*, 2334−2375.
(2) Robson, R. *J. Chem. Soc., Dalton Trans.* **2000**, 3735−3744.
(3) Hosseini, M. W. *Coord. Chem. Rev.* **2003**, *240*, 157−166.
(4) Hagrman, P. J.; Hagrman, D.; Zubieta, J. *Angew. Chem., Int. Ed.* **1999**, *38*, 2638−2684.
(5) Janiak, C. *Dalton Trans.* **2003**, 2781−2804.
(6) Yaghi, O. M.; O'Keeffe, M.; Ockwig, N. W.; Chae, H. K.; Eddaoudi, M.; Kim, J. *Nature* **2003**, *423*, 705−714.
(7) Eddaoudi, M.; Moler, D. B.; LI, H.; Chen, B.; Reineke, T. M.; O'Keeffe, M.; Yaghi, O. M. *Acc. Chem. Res.* **2001**, *34*, 319−330.
(8) Kondo, M.; Yoshitomi, T.; Seki, K.; Matsuzaka, H.; Kitagawa, S. *Angew. Chem., Int. Ed. Engl.* **1997**, *36*, 1725−1727.
(9) Kondo, M.; Okubo, T.; Asami, A.; Noro, S.-I.; Yoshitomi, T.; Kitagawa, S.; Ishii, T.; Matsuzaka, H.; Seki, K. *Angew. Chem., Int. Ed.* **1999**, *38*, 140−143.
(10) Kondo, M.; Shimamura, M.; Noro, S.; Minakoshi, S.; Asami, A.; Seki, K.; Kitagawa, S. *Chem. Mater.* **2000**, *12*, 1288−1299.
(11) Noro, S.-I.; Kitagawa, S.; Kondo, M.; Seki, K. *Angew. Chem., Int. Ed.* **2000**, *39*, 2082−2084.
(12) Li, H.; Eddaoudi, M.; O'Keeffe, M.; Yaghi, O. M. *Nature* **1999**, *402*, 276−279.
(13) Seki, K.; Mori, W. *J. Phys. Chem. B* **2002**, *106*, 1380−1385.
(14) Seki, K. *Chem. Commun.* **2001**, 1496−1497.
(15) Seki, K.; Takamizawa, S.; Mori, W. *Chem. Lett.* **2001**, 332−333.
(16) Seki, K.; Takamizawa, S.; Mori, W. *Chem. Lett.* **2001**, 122−123.
(17) Eddaoudi, M.; Kim, J.; Rosi, N.; Vodak, D.; Wachter, J.; O'Keeffe, M.; Yaghi, O. M. *Science* **2002**, *295*, 469−472.
(18) Chui, S. S.-Y.; Lo, S. M.-F.; Charmant, J. P. H.; Orpen, A. G.; Williams, I. D. *Science* **1999**, *283*, 1148−1150.
(19) Tabares, L. C.; Navarro, J. A. R.; Salas, J. M. *J. Am. Chem. Soc.* **2001**, *123*, 383−387.
(20) Soldatov, D. V.; Ripmeester, J. A. *Chem. Mater.* **2000**, *12*, 1827−1839.
(21) Eddaoudi, M.; Li, H.; Yaghi, O. M. *J. Am. Chem. Soc.* **2000**, *122*, 1391−1397.
(22) Mori, W.; Hoshino, H.; Nishimoto, Y.; Takamizawa, S. *Chem. Lett.* **1999**, 331−332.
(23) Chae, H. K.; Siberio-Pérez, D. Y.; Kim, J.; Go, Y.; Eddaoudi, M.; Matzger, A. J.; O'Keeffe, M.; Yaghi, O. M. *Nature* **2004**, *427*, 523−527.
(24) Rosi, N. L.; Eckert, J.; Eddaoudi, M.; Vodak, D. T.; Kim, J.; O'Keeffe, M.; Yaghi, O. M. *Science* **2003**, *300*, 1127−1129.
(25) Forster, P. M.; Eckert, J.; Chang, J.-S.; Park, S.-E.; Férey, G.; Cheetham, A. K. *J. Am. Chem. Soc.* **2003**, *125*, 1309−1312.
(26) Férey, G.; Latroche, M.; Serre, C.; Millange, F.; Loiseau, T.; Percheron-Guegan, A. *Chem. Commun.* **2003**, 2976−2977.
(27) Dybtsev, D. N.; Chun, H.; Yoon, S. H.; Kim, D.; Kim, K. *J. Am. Chem. Soc.* **2004**, *126*, 32−33.
(28) Fujita, M.; Kwon, J. Y.; Washizu, S.; Ogura, K. *J. Am. Chem. Soc.* **1994**, *116*, 1151−1152.
(29) Seo, J. S.; Whang, D.; Lee, H.; Jun, S. I.; Oh, J.; Jeon, Y. J.; Kim, K. *Nature* **2000**, *404*, 982−986.
(30) Evans, O. R.; Ngo, H. L.; Lin, W. *J. Am. Chem. Soc.* **2001**, *123*, 10395−10396.
(31) Tanski, J. M.; Wolczanski, P. T. *Inorg. Chem.* **2001**, *40*, 2026−2033.
(32) Gomez-Lor, B.; Gutiérrez-Puebla, E.; Iglesias, M.; Monge, M. A.; Ruiz-Valero, C.; Snejko, N. *Inorg. Chem.* **2002**, *41*, 2429−2432.
(33) Tannenbaum, R. *Chem. Mater.* **1994**, *6*, 550−555.

three-dimensional frameworks that do not contain any guest molecules to obtain a porous functionality.[6] This discovery of a second characteristic of coordination polymers has led to the phenomenon being labeled, "second generation compounds".[34] It is believed that a robustness of the host porous framework is a prerequisite for their successful performance, while flexibility is incompatible with the porous properties because it would lead to a collapse of the framework.

On the other hand, bioenzymes, such as metalloproteins, take advantage of their structural flexibility, which appears to be essential for their superb molecular recognition capability. Induced fit theory illustrates the high selectivity in the binding of a substrate to an enzyme, which undergoes conformational change to suite the molecular shape.[35] Therefore, for porous coordination polymers, we also expect that a host flexibility, the so-called "structural dynamism", would be a key principle for high selectivity recognition, accommodation, and separation of a target molecule, which, at present, is regarded as a new class of practical materials.[19−21,36−48] To date, a guideline for obtaining rigid pores in coordination polymers is that stiff building units are linked via strong chemical bonds, such as coordination and/or covalent bonds, to form a 3-D framework. On the other hand, dynamic pores are subject to another guideline to obtain a flexible framework, i.e., that flexible building units (or motifs) are linked via strong bonds, or stiff building blocks (or motifs) are connected via weak bonds. Another possible option is the combination of flexible building blocks (motifs) and weak linkages. The creation of a host framework that can interact with guest species in a switchable fashion has implications for the generation of previously undeveloped advanced materials with potential applications in molecular sensing. For weak linkages, guest molecules readily give rise to changes in the bond direction and distance or to cleavage of bonds.[48] It is worth noting that even weak interactions between the guest molecules and pore-wall molecules can induce a structural change because of the cooperative effect arising from a large ensemble over an infinite framework.[37,49] Since coordination polymers readily form infinite networks, this extended cooperativity would be expected to occur between the molecules throughout the crystal, such that rearrangement could occur in a well-concerted fashion to maintain the macroscopic integrity. Recently, there have been reports on dynamic porous coordination polymers, where simple swollen pores on guest molecule inclusion or shrunken pores on guest molecule exclusion have been realized.[48−64]

Scheme 1

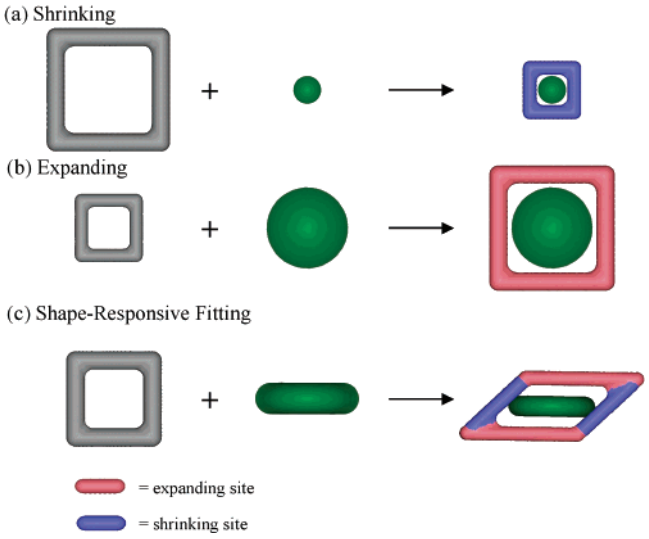

Two fundamental operations for pore deformation, shrink and expansion, are prerequisites for the effective accommodation of a guest molecule. Scheme 1 shows several cases of guest accommodation. Shrinkage (Scheme 1a) occurs on guest molecule inclusion and gives rise to a pore that is well suited to the size and shape of the guest molecule, and therefore, short-range attractive interactions work effectively. To date, a few shrinkable porous coordination polymers have been synthesized where hydrogen bonds between a guest molecule and a host framework occur.[65−67] On the other hand, expansion (Scheme 1b) can also make a guest molecule fit tightly into the host when the size of the pore is smaller than the guest molecule. For guest recognition, simultaneous coupled "shrink and expansion" processes are much more important than either of these process alone. This is a sort of induced fit, in this field, so-called "shape-

(34) Kitagawa, S.; Kondo, M. *Bull. Chem. Soc. Jpn.* **1998**, *71*, 1739−1753.
(35) Davis, A. M.; Teague, S. J. *Angew. Chem., Int. Ed.* **1999**, *38*, 736−749.
(36) We call these flexible porous coordination polymers "third generation compounds".[34]
(37) Uemura, K.; Kitagawa, S.; Fukui, K.; Saito, K. *J. Am. Chem. Soc.* **2004**, *126*, 3817−3828.
(38) Noro, S.; Kitaura, R.; Kondo, M.; Kitagawa, S.; Ishii, T.; Matsuzaka, H.; Yamashita, M. *J. Am. Chem. Soc.* **2002**, *124*, 2568−2583.
(39) Uemura, K.; Kitagawa, S.; Kondo, M.; Fukui, K.; Kitaura, R.; Chang, H.-C.; Mizutani, T. *Chem. Eur. J.* **2002**, *8*, 3587−3600.
(40) Li, H.; Eddaoudi, M.; Groy, T. L.; Yaghi, O. M. *J. Am. Chem. Soc.* **1998**, *120*, 8571−8572.
(41) Li, H.; Davis, C. E.; Groy, T. L.; Kelley, D. G.; Yaghi, O. M. *J. Am. Chem. Soc.* **1998**, *120*, 2186−2187.
(42) Choi, H. J.; Lee, T. S.; Suh, M. P. *Angew. Chem., Int. Ed.* **1999**, *38*, 1405−1408.
(43) Min, K. S.; Suh, M. P. *Chem. Eur. J.* **2001**, *7*, 303−313.
(44) Maspoch, D.; Ruiz-Molina, D.; Wurst, K.; Domingo, N.; Cavallini, M.; Biscarini, F.; Tejada, J.; Rovira, C.; Veciana, J. *Nature Mater.* **2003**, *2*, 190−195.
(45) Carlucci, L.; Ciani, G.; Moret, M.; Proserpio, D. M.; Rizzato, S. *Angew. Chem., Int. Ed.* **2000**, *39*, 1506−1510.
(46) Li, D.; Kaneko, K. *Chem. Phys. Lett.* **2001**, *335*, 50−56.
(47) Rosi, N.; Eddaoudi, M.; Kim, J.; O'Keeffe, M.; Yaghi, O. M. *Angew. Chem., Int. Ed.* **2002**, *41*, 284−287.
(48) Cussen, E. J.; Claridge, J. B.; Rosseinsky, M. J.; Kepert, C. J. *J. Am. Chem. Soc.* **2002**, *124*, 9574−9581.
(49) Kitaura, R.; Seki, K.; Akiyama, G.; Kitagawa, S. *Angew. Chem., Int. Ed.* **2003**, 428−431.
(50) Kitaura, R.; Fujimoto, K.; Noro, S.; Kondo, M.; Kitagawa, S. *Angew. Chem., Int. Ed.* **2002**, *41*, 133−135.
(51) Biradha, K.; Fujita, M. *Angew. Chem., Int. Ed.* **2002**, *41*, 3392−3395.
(52) Beauvais, L. G.; Shores, M. P.; Long, J. R. *J. Am. Chem. Soc.* **2000**, *122*, 2763−2772.
(53) Biradha, K.; Hongo, Y.; Fujita, M. *Angew. Chem., Int. Ed.* **2002**, *41*, 3395−3398.
(54) Suh, M. P.; Ko, J. W.; Choi, H. J. *J. Am. Chem. Soc.* **2002**, *124*, 10976−10977.
(55) Kepert, C. J.; Hesek, D.; Beer, P. D.; Rosseinsky, M. J. *Angew. Chem., Int. Ed.* **1998**, *37*, 3158−3160.
(56) Soldatov, D. V.; Ripmeester, J. A.; Shergina, S. I.; Sokolov, I. E.; Zanina, A. S.; Gromilov, S. A.; Dyadin, Y. A. *J. Am. Chem. Soc.* **1999**, *121*, 4179−4188.
(57) Lu, J. Y.; Babb, A. M. *Chem. Commun.* **2002**, 1340−1341.
(58) Abrahams, B. F.; Jackson, P. A.; Robson, R. *Angew. Chem., Int. Ed.* **1998**, *37*, 2656−2659.
(59) Fletcher, A. J.; Cussen, E. J.; Prior, T. J.; Rosseinsky, M. J.; Kepert, C. J.; Thomas, K. M. *J. Am. Chem. Soc.* **2001**, *123*, 10001−10011.
(60) Kepert, C. J.; Rosseinsky, M. J. *Chem. Commun.* **1999**, 375−376.
(61) Seki, K. *Phys. Chem. Chem. Phys.* **2002**, *4*, 1968−1971.
(62) Takamizawa, S.; Nakata, E.-i.; Yokoyama, H.; Mochizuki, K.; Mori, W. *Angew. Chem., Int. Ed.* **2003**, *42*, 4331−4334.
(63) Makinen, S. K.; Melcer, N. J.; Parvez, M.; Shimizu, G. K. H. *Chem. Eur. J.* **2001**, *7*, 5176−5182.
(64) Liao, J.-H.; Cheng, S.-H.; Su, C.-T. *Inorg. Chem. Commun.* **2002**, *5*, 761−764.
(65) Barthelet, K.; Marrot, J.; Riou, D.; Férey, G. *Angew. Chem., Int. Ed.* **2002**, *41*, 281−284.
(66) Serre, C.; Millange, F.; Thouvenot, C.; Nogues, M.; Marsolier, G.; Louer, D.; Férey, G. *J. Am. Chem. Soc.* **2002**, *124*, 13519−13526.
(67) Maji, T. K.; Uemura, K.; Chang, H.-C.; Matsuda, R.; Kitagawa, S. *Angew. Chem., Int. Ed.* **2004**, *43*, 3269−3272.

responsive fitting". To realize a "shape-responsive fitting pore", a porous framework has to be able to deform its structure using both expansion and shrinkage to accommodate a guest molecule effectively (Scheme 1c). In this context, it is of significance to design and prepare a structure that can both shrink and expand in response to the presence and absence of a guest molecule.

A porous coordination polymer with pillared layer structure (CPL) ($[Cu_2(pzdc)_2(bpy)]$ (**CPL-2**) (pzdc = pyrazine-2,3-dicarboxylate, bpy = 4,4′-bipyridine)[9] was constructed from stiff motifs of bpy and the pyrazine ring in pzdc, a flexible motif of the carboxyl groups with the rotational freedom, and a copper ion geometry that possesses a degree of flexibility in bond cleavage due to the Jahn−Teller distortion. Therefore, **CPL-2** is a good representative of a flexible framework, affording an unprecedented guest shape and size responsive fitting capability.

For our work, we chose **CPL-2** as the host porous framework and benzene as the guest molecule, as the nonspherical shape of the guest molecule would clearly amplify any "shape-responsive fitting" aspect of the flexible pore. We have demonstrated the reversible structural change on guest molecule adsorption/desorption by monitoring the resulting X-ray diffraction patterns, which detected a "shape-responsive fitting" profile on guest molecule adsorption with large crystalline shrinking.

Experimental Section

Synthesis of $\{[Cu_2(pzdc)_2(bpy)]\cdot 4H_2O\}$ (CPL-2 ⊃ H_2O). A mixture solution of Na_2pzdc (0.21 g, 1.00 mmol) and bpy (0.078 g, 0.50 mmol) dissolved in H_2O/EtOH (1/1) was slowly added to the H_2O solution (100 mL) containing $Cu(ClO_4)_2\cdot 6H_2O$ (0.37 g, 1.00 mmol) at room temperature. After being stirred for 1 day, the resultant precipitate was filtered, washed with H_2O and methanol, and dried under reduced pressure.

Adsorption Measurements. The adsorption isotherms of benzene at 300 K, nitrogen at 77 K, and water at 300 K were measured with BELSORP18 volumetric adsorption equipment from Bel Japan, Inc. Benzene was purchased from Wako Pure Chemical Industries, Ltd. Nitrogen gas of high purity (99.9999%) was used. Prior to the adsorption measurements, benzene and water were degassed by five freeze−thaw evacuation cycles, and the **CPL-2** host sample (**apohost**) was obtained by treatment under reduced pressure ($<10^{-2}$ Pa) at 378 K for more than 10 h.

X-ray Powder Diffraction (XRPD) Experiment. The powder samples for each compound were sealed in a silica glass capillary (0.4 mm inside diameter). XRPD pattern with good counting statistics was measured by the synchrotron radiation XRPD experiment with the large Debye−Scherrer camera and imaging plate as detectors on the BL02B2 beam line at the Super Photon Ring (SPring-8, Hyogo, Japan).[68] All the XRPD patterns are obtained with a 0.01° step.

Structure Determination. The structure determinations were performed using a high brilliance synchrotron powder diffraction data. The patterns were indexed by using the indexing program DICVOL91.[69] A good quality unit cell refinement was obtained by using the structureless Le Bail fitting method.[70] The FOX software, which combines a rigid body and a Monte Carlo approach in the real space, was used to find the initial positions of atoms for Rietveld analysis.[71] The final structures were refined by Rietveld technique.[72,73] The wavelength of incident X-rays, 2θ range and number of reflections for calculation are summarized in Table 3. For the **apohost,** the preliminary structure model was constructed from **CPL-1** $\{[Cu_2(pzdc)_2(pyz)]\cdot 4H_2O\}$ (pyz = pyrazine) of isostructural crystal, whose structure was determined by X-ray crystal structure analysis using a single-crystal sample.[9] For the **CPL-2 ⊃ benzene**, we tried to find the preliminary structure model by Fox software. After calculation, we got the two preliminary structure models of **CPL-2 ⊃ benzene**; one model has one site for benzene molecule with full occupancy in each unit pore (one-site model) and another model has two sites for benzene molecules with half occupancies in each unit pore (two-site model). Both structure models were analyzed by Rietveld method. As a result, using the two-site model, the two benzene molecules approach each other and tend to overlap, which means the two-site structure model provides a one-site model eventually. Therefore, the two-site model was excluded and then the one-site model was well refined.

Results and Discussion

Sorption Properties. The adsorption isotherms of nitrogen, benzene, and water on the **apohost** were measured at 77, 300, and 300 K, respectively, and are shown in Figure 1. The nitrogen adsorption isotherm is a typical Type I adsorption isotherm as defined by the IUPAC classification scheme,[74] confirming the presence of micropores without any mesopores in the sample. This agrees with the isotherm reported by Kaneko et al.[75] in regard to their profile and onset of adsorption pressure. The benzene adsorption isotherm also shows a typical Type I behavior, indicating that the effective micropore filling occurs for benzene. Micropore filling occurred at very low P/P_0 region, indicating enhanced adsorbent−adsorbate interaction. On the other hand, water adsorption occurred at higher P/P_0 region than for benzene adsorption, indicating that the strength of the adsorbate−adsorbate interaction relative to the apohost−adsorbate interaction was higher when the adsorbate was water versus the case where the adsorbate was benzene. In addition, after an initial abrupt adsorption up to about four molecules per the unit pore, any further water adsorption occurred gradually, while little benzene adsorption occurred after the initial abrupt adsorption, which is interpreted as suggesting that for water molecules, the apohost possessed other weaker adsorption sites than the initial adsorption sites, or that the adsorbed water molecules undergo a rearrangement after the initial adsorption, which allowed for further adsorption. These results indicate **CPL-2** did not provide a simple adsorption site for water molecules, which may be ascribed to the two types of areas in a unit pore: one being hydrophobic, and the other being hydrophilic.

A marked difference in the nitrogen and benzene adsorption isotherms was also observed. The adsorbed amount of benzene is saturated at just one molecule per unit pore, whereas that of nitrogen indicated a nonintegral value (3.2 at $P/P_o = 0.2$, and 3.7 at $P/P_o = 0.9$). Another difference was observed in plots of the logarithm of the relative pressure, as shown in parts b and d of Figure 1. The nitrogen isotherm exhibited several steps in the range $P/P_o = 1.0 \times 10^{-5} - 1.0 \times 10^{-1}$, while benzene isotherm exhibited a single clear step at $P/P_o = 2.0 \times 10^{-3}$.

These differences can be accounted for by the degree of matching of the size and shape (i.e., structural dimensions) of

(68) Nishibori, E.; Takata, M.; Kato, K.; Sakata, M.; Kubota, Y.; Aoyagi, S.; Kuroiwa, Y.; Yamakata, M.; Ikeda, N. *J. Phys. Chem. Solid* **2001**, *62*, 2095−2098.
(69) Boultif, A.; Louer, D. *J. Appl. Crystallogr.* **1991**, *24*, 987−993.
(70) LeBail, B.; Duroy, H.; Fourquet, J. L. *Mater. Res. Bull.* **1988**, *23*, 447−452.
(71) Favre-Nicolin, V.; Ćerný, R. *J. Appl. Crystallogr.* **2002**, *35*, 734−743.
(72) Rietveld, H. M. *J. Appl. Crystallogr.* **1969**, *2*, 65−71.
(73) Izumi, F.; Ikeda, T. *Mater. Sci. Forum* **2000**, *198*, 321−324.
(74) Rouquerol, F.; Rouquerol, J.; Sing, K. *Adsorption by Powders and Porous Solids*; Academic Press: London, 1999.
(75) Li, D.; Kaneko, K. *J. Phys. Chem. B* **2000**, *104*, 8940−8945.

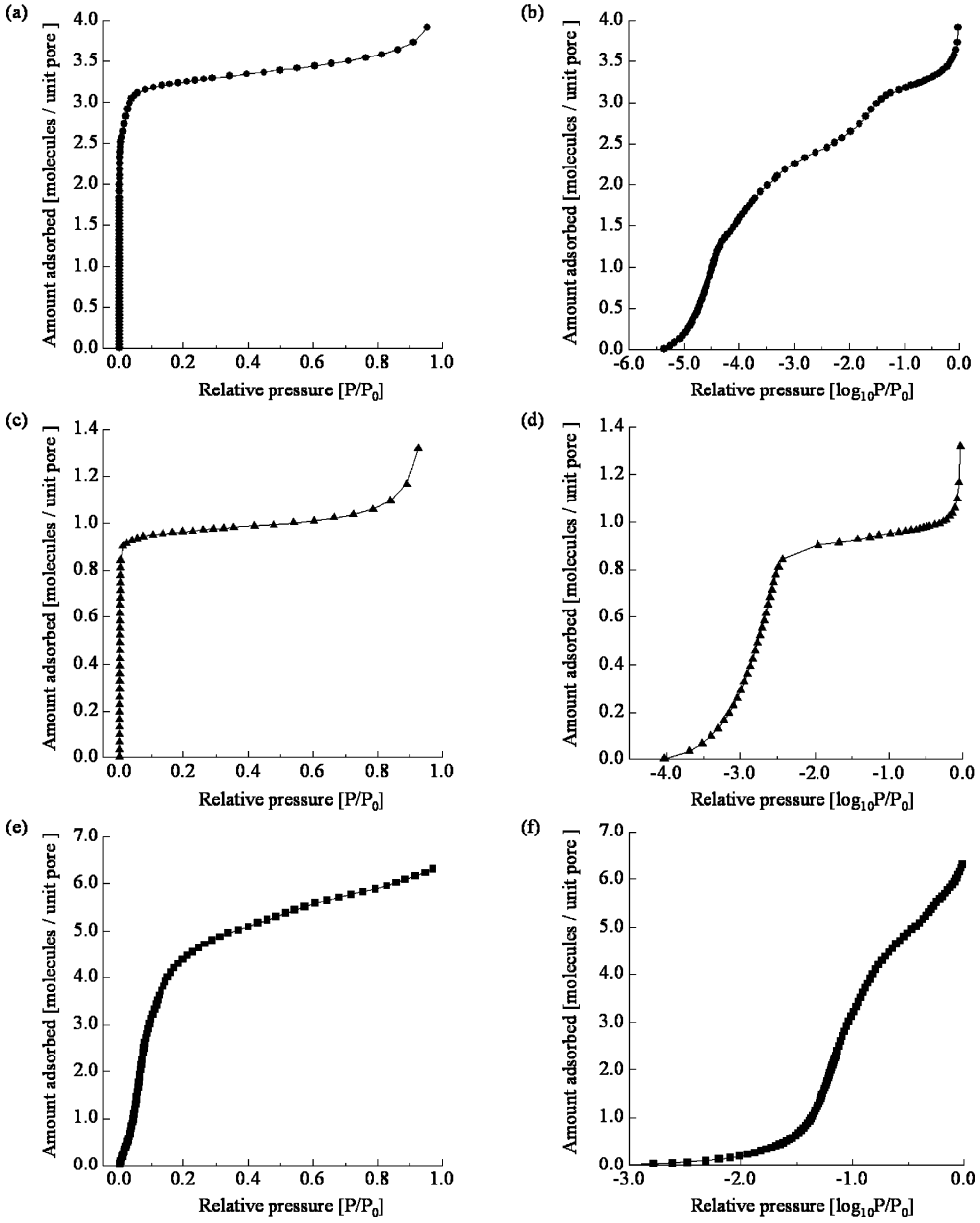

Figure 1. (a) Adsorption isotherm for nitrogen of **CPL-2** at 77 K in the relative pressure range from 10^{-6} to 0.95. P_0 is the saturated vapor pressure, 101 kPa of nitrogen at 77 K. (b) Adsorption isotherms for nitrogen at 77 K plotted against a logarithmic relative pressure. (c) Adsorption isotherm for benzene of **CPL-2** at 300 K in the relative pressure range from 10^{-4} to 0.95. P_0 is the saturated vapor pressure, 14.6 kPa, of benzene at 300 K. (d) Adsorption isotherms for benzene at 300K plotted against a logarithmic relative pressure. (e) Adsorption isotherm for water of **CPL-2** at 300 K in the relative pressure range from 10^{-3} to 1.0. P_0 is the saturated vapor pressure, 3.53 kPa, of water at 300 K. (f) Adsorption isotherms for water at 300K plotted against a logarithmic relative pressure.

the adsorbate with those of the channel unit, the so-called commensurability. The regularity of the channels produces an attractive periodic potential, in which the guest molecules are confined to each unit pore.[76] The better a guest molecule is suited to a unit pore, then the more effective the confinement is.[77] Compared to benzene, nitrogen molecules are almost spherical adsorbate (dimensions = 3.0 Å × 3.0 Å × 4.0 Å), whereas benzene molecules are anisotropic (i.e., a flattened shape) with dimensions = 3.3 Å × 6.6 Å × 7.3 Å.[78] When an integral number of guest molecules can be densely packed within a given periodic unit pore, then the structures for both the host and guest molecules would be matched from the periodicity. In the case of benzene, only one molecule can be accommodated in a unit pore of the channel, in a so-called "commensurate fashion". On the other hand, nitrogen is so small that a size mismatch occurs, and a nonintegral number of molecules can be packed in a unit pore. Interestingly, the channels have several sites with a different affinity for nitrogen, ascribing a multifunctionality on the channel walls. As a result, **CPL-2** affords single pockets in the "unit pore" for benzene (commensurate adsorption), whereas several it has nonidentical pockets in the "unit pore" for nitrogen (incommensurate adsorption). Accordingly, the commensurate array of benzene molecules in the

(76) Kitaura, R.; Kitagawa, S.; Kubota, Y.; Kobayashi, T. C.; Kindo, K.; Mita, Y.; Matsuo, A.; Kobayashi, M.; Chang, H.-C.; Ozawa, T. C.; Suzuki, M.; Sakata, M.; Takata, M. *Science* **2002**, *298*, 2358−2361.
(77) Jobic, H.; Methivier, A.; Ehlers, G.; Farago, B.; Haeussler, W. *Angew. Chem., Int. Ed.* **2004**, *43*, 364−366.
(78) Webster, C. E.; Drago, R. S.; Zerner, M. C. *J. Am. Chem. Soc.* **1998**, *120*, 5509−5516.

Table 1. Micropore Parameters of **CPL-2** by Nitrogen and Benzene Adsorptions from DR Analysis

adsorbate (*T*/K)	W_o (cm^3 (STP)g^{-1})	V_m (cm^3 g^{-1})	βE_o (kJ mol^{-1})	$q_{st,\Phi=1/e}$ (kJ mol^{-1})
nitrogen (77)	114	0.176	7.45	13.0
benzene (300)	35.4	0.142	38.0	70.0

channel is preferentially accommodated in the new crystalline phase unlike the precursor form without a guest molecule.

Dubinin−Radushkevich (DR) equation was used to analyze the resulting isotherms and to characterize the porous properties of **CPL-2**. The DR equation is given by

$$\ln W = \ln W_o + (A/\beta E_o)^2 \quad (1)$$

where W and W_o are the amount of adsorption at a relative pressure (P/P_o) and the saturated amount of adsorption, respectively, E_o is a characteristic adsorption energy, and the parameter A is Polanyi's adsorption potential, defined as $A = RT \ln(P_o/P)$.[79] The parameter β is the affinity coefficient and is related to the adsorbate−adsorbent interaction. The DR plots showed a linear relationship existed at higher P/P_o region, from which the micropore volume and the value of βE_o were obtained in Table 1. The micropore volume, V_m, was calculated from the value of W_o and the density of the adsorbate by assuming that the molecules were adsorbed as a liquid. Furthermore, the value of βE_o allows for the calculation of the isosteric heat of adsorption, $q_{st,\Phi=1/e}$, at the fractional filling of $1/e$ using eq 2 where ΔH_v is the heat of vaporization of the bulk liquid. The values for ΔH_v for nitrogen at 77 K and benzene at 300 K are 5.58 and 32 kJ mol^{-1}, respectively.

$$q_{st,\Phi=1/e} = \Delta H_v + \beta E_o \quad (2)$$

Table 1 shows that the values of $q_{st,\Phi=1/e}$ for nitrogen and for benzene on **CPL-2** are larger than those of activated carbon (~12 and ~55 kJ/mol, respectively).[80,81] The values of V_m obtained for benzene and nitrogen are different, with the value estimated for benzene of $V_m = 0.142$ cm^3 g^{-1} being is smaller by 19% than that of nitrogen, 0.176 cm^3 g^{-1}. This is attributed to two factors: (i) benzene molecules being unable to fill the initial void space sufficiently, resulting in a low space-filling ratio and, therefore, a low estimated V_m, and (ii) a structural transformation taking place, which, for example, would cause a marked shrinkage of the pores for benzene and an eventual smaller value of V_m than that of nitrogen.

The space-filling ratio of the micropore is sensitive to the geometry of the adsorbate molecules.[75] Although factor (i) above could be a main reason for the observed data, at present, we do not have any reason to avoid supposing that factor (ii) is applicable, because **CPL-2** has a flexible framework. To confirm the contribution of factor (ii) to the data, we carried out direct observations on the structural changes utilizing X-ray crystallography in the presence and absence of guest molecules.

Unit Cell Contraction. The XRPD patterns at 300 K of as-synthesized **CPL-2 (CPL-2 ⊃ H_2O)**, anhydrous **CPL-2** without a guest molecule (**apohost**) under reduced pressure, and **CPL-2** with benzene (**CPL-2 ⊃ benzene**) at 1.0 kPa (a relative pressure of about 0.07) are shown in Figure 2. After dehydration[82] of the **CPL-2 ⊃ H_2O**, a slight change was observed in the peak positions, while an appreciable change in intensity was seen. On the other hand, after exposure to benzene vapor, a marked change took place in both peak position and intensity. In particular, the 020 peak at the lowest 2θ value moved to a higher angle region, which is indicative of a contraction in structure. Interestingly, the XRPD pattern of **CPL-2 ⊃ benzene** returned to that of the guest-free structure after removal of the benzene by heating the sample at 373 K under reduced pressure, indicating that this structural transformation is reversible. We examined this lattice contraction in detail, and obtained good quality unit cell parameters from each of the powder diffraction traces shown in Figure 2, using the structureless Le Bail fitting method.[70] The final fitting values are shown in Table 2. The space group for all the samples was assigned as $P2_1/c$. On removal of the guest−water molecules from **CPL-2 ⊃ H_2O**, the b axis and the unit cell volume decreased by 0.82% and 2.5%, respectively. Such a structural contraction in metal-organic porous compounds is quite common after removal of the guest molecules, as well as in **CPL-1** with an isostructural porous

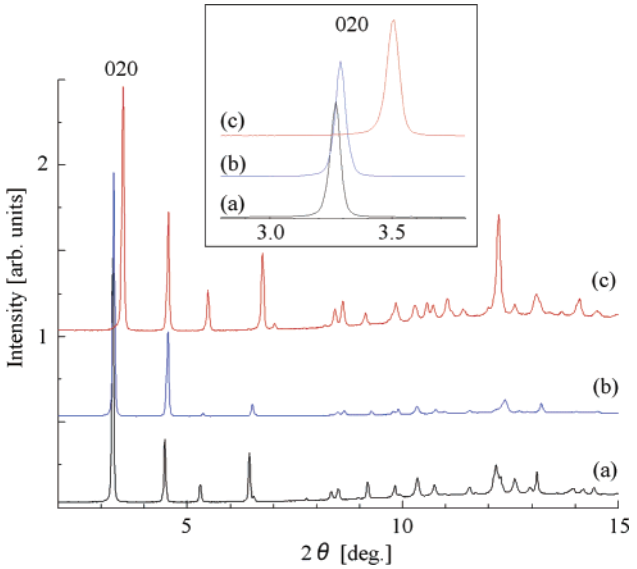

Figure 2. Synchrotron XRPD patterns at 300 K of (a) **CPL-2 ⊃ H_2O**, which contains water molecules as guests, (b) **apohost** under reduced pressure, and (c) **CPL-2 ⊃ benzene** at 1.0 kPa vapor pressure of benzene. The radiation wavelength is 0.80087 Å and the 2θ ranges from 2° to 15°. Inset shows the peak 020 at the lowest 2θ in the range of 2.8° to 3.8°.

Table 2. Crystallographic Data for **CPL-2 ⊃ H_2O**, **Apohost**, and **CPL-2 ⊃ Benzene**

	CPL-2 ⊃ H_2O	apohost	CPL-2 ⊃ benzene
crystal system	monoclinic	monoclinic	monoclinic
space group	$P2_1/c$	$P2_1/c$	$P2_1/c$
a^a (Å)	4.7143(13)	4.7177(2)	4.7714(13)
b^a (Å)	28.0546(4)	27.827(12)	26.0665(5)
c^a (Å)	11.0728(3)	10.8770(4)	10.9589(2)
β^a (deg)	96.289(3)	96.017(5)	96.567(3)
V^a (Å^3)	1455.69(6)	1420.05(8)	1354.05(5)
radiation (Å)	0.80087	0.80087	0.80087
T (K)	300(5)	300(5)	300(5)

[a] The unit cell parameters are refined by structureless LeBail pattern fitting analysis.

(79) Dubinin, M. M. *Chem. Rev.* **1960**, *60*, 235−241.
(80) Kaneko, K.; Shimizu, K.; Suzuki, T. *J. Chem. Phys.* **1992**, *97*, 8705−8711.
(81) Dubinin, M. M. *Carbon* **1987**, *25*, 593−598.
(82) **CPL-2 ⊃ H_2O** sample is completely dehydrated at 393 K under reduced pressure.

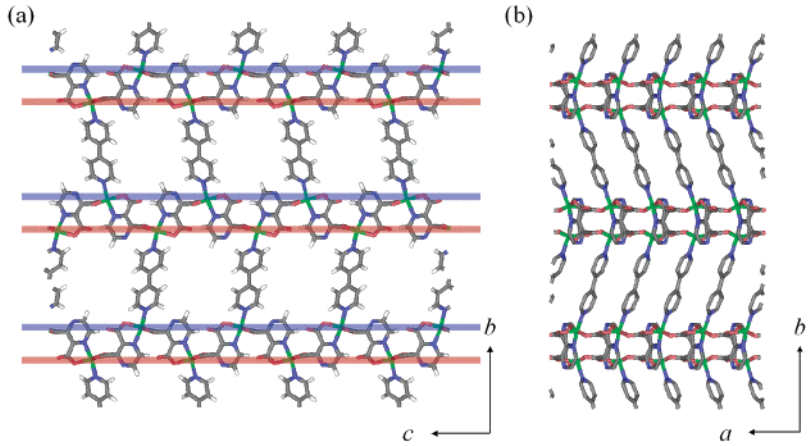

Figure 3. Crystal structure of $[Cu_2(pzdc)_2(bpy)]_n$ (**apohost**). (a) Crystal view of **apohost** along the *a* axis. Blue and red lines indicate the copper atom sheets projected down to the *a* axis, which practically forms layers. (b) Crystal view of **apohost** along the *c* axis. Hydrogen atoms are omitted for clarity.

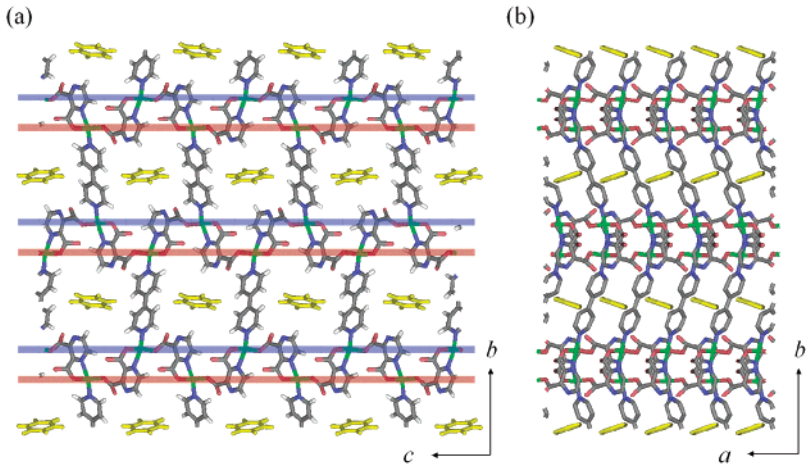

Figure 4. Crystal structure of $\{[Cu_2(pzdc)_2(bpy)]\cdot C_6H_6\}_n$ (**CPL-2 ⊃ benzene**). The benzene molecules are located in the each channel. (a) Crystal view of **CPL-2 ⊃ benzene** along the *a* axis. Blue and red lines indicate the copper atom sheets projected down to the *a* axis, which practically form layers. (b) Crystal view of **CPL-2 ⊃ benzene** along the *c* axis. Hydrogen atoms are omitted for clarity.

Table 3. Crystallographic Data and Rietveld Refinement Summary for **Apohost** at 293 K and **CPL-2 ⊃ Benzene** at 273 K

	apohost	CPL-2 ⊃ benzene
chemical formula	$C_{11}H_6CuN_3O_4$	$C_{14}H_9CuN_3O_4$
formula weight	303.77	346.79
crystal system	monoclinic	monoclinic
space group	$P2_1/c$	$P2_1/c$
a (Å)	4.71160(3)	4.7729(6)
b (Å)	27.833(16)	26.040(12)
c (Å)	10.8881(6)	10.9488(8)
β (deg)	96.0102(6)	96.61(10)
V (Å^3)	1421.09(15)	1351.7(2)
Z	4	4
radiation (Å)	0.80092	0.80087
2θ range	$1.90° < 2\theta < 36.00°$	$2.80° < 2\theta < 35.00°$
T (K)	293(5)	273(5)
no. of reflections	713	656
R_{wp}[a]	0.0415	0.0503
R_I[b]	0.0456	0.0467

[a] $R_{wp} = [\Sigma w(|y_o| - |y_c|)^2/\Sigma w y_o^2]^{1/2}$. [b] $R_I = \Sigma(||I_o| - |I_c||)/\Sigma|I_o|$.

coordination polymer.[76] Surprisingly, further decrease of the unit cell dimensions was identified when benzene molecules were adsorbed on the **apohost**. A large reduction in the *b* axis and unit cell volume was observed of 6.8% and 4.9%, respectively, even though the benzene molecules were present in the channels.

Micropore Structures of the Apohost and CPL-2 ⊃ Benzene. The crystal structures of the **apohost** at 293 K and **CPL-2 ⊃ benzene** at 273 K were determined from XRPD

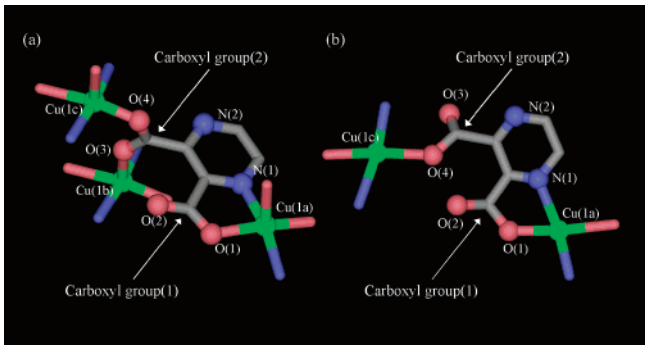

Figure 5. Crystal structures around the pzdc ligand of (a) **apohost** and (b) **CPL-2 ⊃ benzene** (Cu, green; O, pink; N, blue; C, gray). Hydrogen atoms are omitted for clarity.

measurements and Rietveld analysis. The final crystallographic data and the reliability factors of the Rietveld analysis (R_I and R_{wp}) are shown in Table 3. Figures 3 and 4 show the full crystal structures of the **apohost** at 293 K and **CPL-2 ⊃ benzene** at 273 K, respectively.

In **apohost** structure, the pzdc units link the three crystallographically equivalent copper atoms (Cu(1a), Cu(1b), and Cu(1c)), as shown in Figure 5(a). The N(1) and O(1) atoms of carboxyl group(1) chelates with the Cu(1a) atom.The carboxyl group(2) bridges Cu(1b) and Cu(1c) atoms in such a fashion

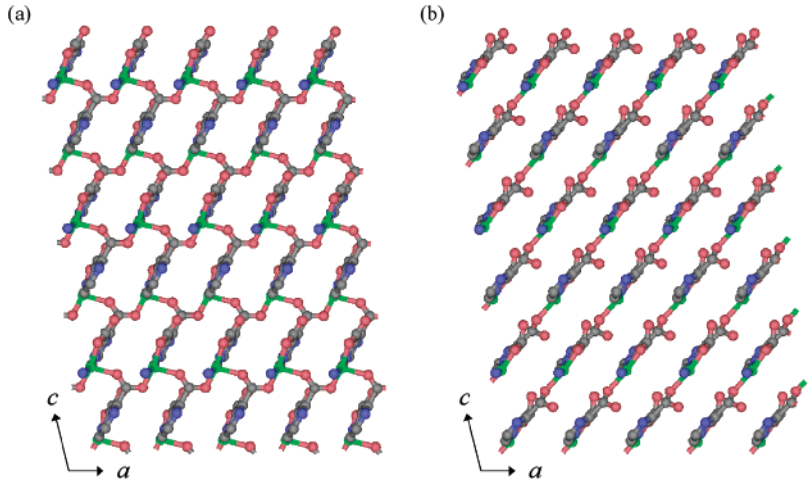

Figure 6. Views of the two-dimensional layers of (a) **apohost** and (b) **CPL-2 ⊃ benzene**.

that the O(3) and O(4) atoms are sited at the apical and equatorial positions, respectively. The remaining N(2) and O(2) atoms have no interaction with any other atoms. As a result, a neutral two-dimensional layer of $[Cu(pzdc)]_n$ forms in the *ac* plane, as shown in Figure 6a. These layers are connected by bpy groups acting as pillar ligands, resulting in a 3D pillared layer structure, as shown in Figure 3.

The coordination manner in the structure of **CPL-2 ⊃ benzene**, as shown in Figure 5b, is similar to the **apohost** structure, except for one difference: the O(3) atom of carboxyl group(2) is dissociated, and a subsequent rotation of carboxyl group(2) occurs. As a result, chain motifs of (Cu/pzdc) running along the $(a + c)$ vector are aligned in a parallel fashion to form "layers" forms, as shown in Figure 6b. These "layers" are linked by bpy groups acting as pillar ligands to afford a pillared layer structure, similar to that of **apohost**. The guest benzene molecule are located in the channels surrounded by the four pillar ligands, as indicated by the adsorption saturation number of one molecule per unit pore, which is in good agreement with the value obtained from the adsorption isotherm, as shown in Figure 4. The surface of each bpy pillar ligand has a slight curvature due to its molecular shape, so that the four pillar ligands provide a hollow in the middle of the channel. Therefore, the benzene molecule is located in this hollow, which means that the pore shape is suitable for fixing a benzene molecule.

Flexible Pore Structure Suited for Benzene. Both the **CPL-2 ⊃ benzene** and the **apohost** structures possess 1D channels running along the *a* axis, based on the pillared layer form. Interestingly, the pillared layer framework undergoes a deformation such that the channel cavities suit benzene molecules very well, resulting in an appreciable difference in the channel shape for cases with, and without benzene. The channel in the absence of benzene has a near rectangular shape with dimensions of 5.6 Å/7.2 Å,[83] whereas in the presence of benzene the rectangular shape changes to form a shape in the form of a "Z", as shown in Figure 7. The benzene molecules are located in the center of the pores, with the plane of the benzene molecule being surrounded closely by the hydrogen atoms of the pzdc ligands.

(83) The cross-section is not regular square but parallelogram. X Å/Y Å represents lengthes of each side of parallelogram. The size is measured by considering van der Waals radii for constituting atoms.

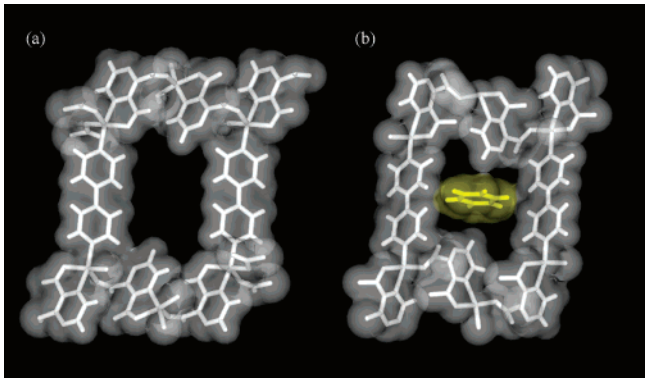

Figure 7. Representation of the pore structures of (a) **apohost** and (b) **CPL-2 ⊃ benzene**. Both of views are down from *a*-axis, displayed by stick and van der Waals surface models.

Careful inspection of the layer structure reveals that the layers are corrugated, as if there existed two sheets from the upper and the lower copper atom assemblies. These two sheets are represented by the red and blue colors in Figures 3, 4, and 8. The pzdc ligands bridging the nearest neighbor Cu atoms sit between the sheets. Interestingly, the Cu sheets in the layer undergo a mutual slide, affording the gap contraction in crystal contraction transformation, especially along the *b* axis (Δb = 1.76 Å). This sheet slide principally arises from the change of the coordination mode of the Cu(II) ions (Figure 8). In the absence of benzene, the geometry around the copper ion is square pyramidal form, with the bond distances between the Cu(II) and apical O atoms being, Cu−O(1) = 2.1 Å and Cu−O(2) = 4.3 Å (Figure 9a) the bond distances while in the presence of benzene show a square planer form with Cu−O(1) = 3.7 Å and Cu−O(2) = 5.0 Å (Figure 9b). Eventually, the deformation produces a large contact area with the benzene plane, and as a result, the pore structure provides a "Z"-shaped pocket that is well suited for accommodating benzene.

Dynamic Profile of CPL-2. Dynamic pores are subject to a guideline for forming a flexible framework in that building units (or motifs) with flexible moieties are linked via strong bonds or stiff building blocks (or motifs) are connected via weaker bonds. These combinations afford a subtly balanced porous framework, namely, a soft framework. Dynamic channels could form from a "soft" framework with bistability, whose two states oscillate between one of the counterparts. Such a system could

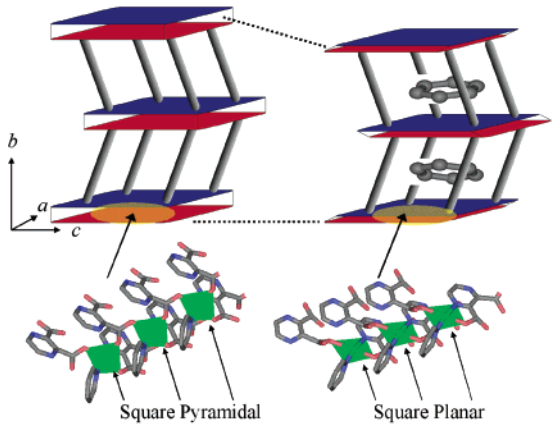

Figure 8. Schematic representation of the structural transformation with "Shape-responsive fitting" triggered by benzene adsorption. The mutual slide of the 2D sheets and the pore shrinking is observed, which is accompanied by the change of the Cu coordination geometry from a square pyramid to a square plane. Two-dimensional sheets of $[Cu(pzcd)]_n$ and the pillar of bpy are represented by blue and red boards and by gray sticks, respectively.

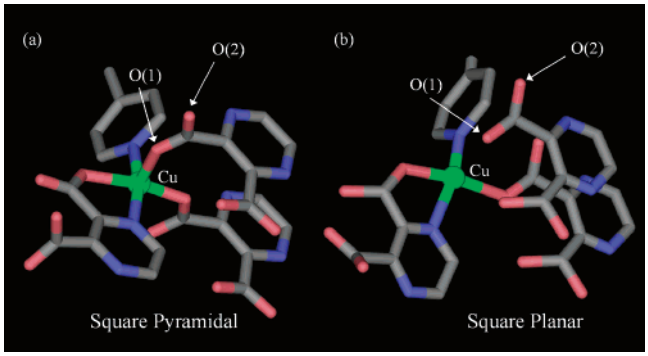

Figure 9. The geometry around the Cu atom; (a) **apohost** indicates a square pyramidal form and (b) **CPL-2** ⊃ **benzene** indicates a square planar form.

exist in one or two states for a given set of external field parameters. The structural rearrangement of this framework would proceed from the "open" phase to the "contracted" phase in response to the presence of a guest molecule. For this phase transition to occur, a certain type of device is indispensable, which is constructed from several components, that we denote as a "Functional Synthon".[1] In the case of **CPL-2**, the components are bpy and pzdc rings as stiff motifs, the rotatable carboxyl groups in pzdc, and the fluxional coordination geometry of the Cu ion, and all provide the contrivance for a unique flexible channel structure. The dynamic structural transformation of **CPL-2** is derived from the change in coordination mode, based on the cleavage of the apical long Cu−O bonds in the Cu geometry and the subsequent rotation of the carboxyl groups. Therefore, we can consider that one of the keys to create a dynamic network system is to use Cu(II) ions in the d^9 configuration, because this provides the best opportunity to observe the Jahn−Teller effect.

Despite there being no specific interaction[84] between the guest molecules and the host framework, a crystal-to-crystal phase transition occurs in our framework. The structural transformation is attributable to the dispersion forces between the benzene molecules and pore walls. Stabilization resulting from the dispersion force between the benzene molecules and the pore walls depends on the interatomic distances. Motions toward shortening these distances have the advantage of increasing the degree of interaction. Therefore, a structural transformation from the "open" phase to the "contracted" phase results in a shortening of interatomic distances between the benzene and the pore walls.

Conclusion

We have carried out in situ XRPD measurements on **CPL-2** under different atmospheric conditions and have determined these structures. Benzene molecules having an anisotropic (nonspherical) shape were utilized to investigate the flexibility of the framework because benzene could not fill all the micropore space and does not show effective adsorption in the rectangular micropore. As a result, we observed a "shape-responsive fitting" type crystal-to-crystal transformation with a large cell contraction. The contraction occurred so that the contact surface area between the benzene molecules and the pore walls, which gives raise to the effective interactions, preferentially increased. The additional interaction energy may compensate for the energy loss from bond cleavage of the copper−oxygen moiety. This aspect could explain the experimental tendencies observed for the micropore volumes and heat of adsorption. The host flexibility improves the efficiency of the adsorption by aiding the host structural transformation suited for incorporating the guest molecules.

Most of the porous materials have been synthesized with the aim of obtaining a robust structure. However, we believe that flexible frameworks provide pore structures that are suited for a given guest molecule and are much more useful for molecular recognition or selective guest inclusion than a robust porous structure. The "shape-responsive fitting" properties afford a novel recognition system using crystalline materials. We expect that these flexible crystalline coordination polymers will open up a new field of porous materials, being the best candidates for a porous material that can recognize and separate target molecules.

Acknowledgment. The synchrotron radiation experiments were performed at the BL02B2 in the SPring-8 with the approval of the Japan Synchrotron Radiation Research Institute (JASRI). Authors thank to Dr. K. Kato for his experimental help at SPring-8. This work was supported by a Grant-In-Aid for Science Research in a Priority Area "Chemistry of Coordination Space" (No. 464) from the Ministry of Education, Science, Sports, and Culture, Japan.

Supporting Information Available: Dubinin−Raduskevich plots of N2 adsorption data; adsorption and desorption isotherms; observed and calculated X-ray powder diffraction patterns. This material is available free of charge via the Internet at http://pubs.acs.org.

JA046925M

(84) Benzene has an electric quadrupole moment that may interact with the anionic oxygen atoms of the carboxyl groups in the pore walls, and in addition, the benzene π electrons may interact with the hydrogen atoms in the pore walls, such as in a CH−π interaction. However, according to the guest-accommodated structure, we could not characterize these interaction sites.